Pergamon

Cement and Concrete Research 29 (1999) 1047–1053

CEMENT AND CONCRETE RESEARCH

A model for the calculation of combined chemical reactions and transport processes and its application to the corrosion of mineral-building materials
Part II. Experimental verification

Frank Schmidt-Döhl*, Ferdinand S. Rostásy

Institut für Baustoffe, Massivbau und Brandschutz, Technische Universität Braunschweig, Beethovenstraße 52, 38106 Braunschweig, Germany

Received 19 September 1997; accepted 26 January 1999

Abstract

A model for the simulation of corrosion processes of mineral building materials is provided. The model combines the calculation of several transport processes with the quantitative simulation of the chemical reactions. The model was verified by experiments on the corrosion of cement mortar by sulfate solutions and acid, the corrosion of cement mortar and concrete in a seepage water treatment plant (ammonium attack), and the corrosion of a sandstone with calcitic binder by acidic solutions with and without sulfate content. The corresponding simulations were calculated using solely the properties of the uncorroded materials (experimentally determined or estimated by the literature). The comparison of the measured and calculated corrosion behaviour lead to the conclusion that the algorithm is able to simulate very different corrosion processes without any change of the model, despite some difficulty in detail.

Keywords: Durability; Modeling

In the first part of this paper, a model for the simulation of corrosion processes of mineral building materials was described [1]. It combines modules for the calculation of the thermodynamic and kinetic stable phase assemblage for the calculation of several transport processes, modules for the actualization of the transport parameters and the material strength, and the calculation of the expansion caused by sulfate attack within a space and time incremental simulation. The model was verified by experiments concerning the corrosion of cement mortar by sulfate solutions, acid, the corrosion of cement mortar and concrete in a seepage water treatment plant (ammonium attack), and the corrosion of a sandstone with calcitic binder by acidic solutions with and without sulfate. We describe the materials and the starting parameters of the simulations. Then the results of the corrosion experiments and the calculated material behaviour are compared. More detailed information about the model and the experiments are described elsewhere [2].

1. Starting values of the simulation program

1.1. Materials and mixture proportions

The mixture proportions of the cement mortar and the concrete used for the corrosion experiments are shown in Table 1. The sandstone consists of quartz-rich components, which are barely in contact with each other. The binder is calcitic (No. 130 in [3]).

1.2. Initial phase assemblage and moisture distribution of the specimens

The mortar specimens were stored at 100% relative humidity and 17–20 °C for 3 months after which all mortar and the sandstone specimens were stored above saturated NaCl solution (75% relative humidity) for at least 3 months until they reached hygric equilibrium. The initial values to calculate the stable phase assemblage of the uncorroded mortar are the mixture proportions (see Table 1), the Bogue calculation of the cement (C_3S, 46.21%; C_2S, 28.54%; C_3A, 9.40%; C_4AF, 5.16%), the degree of hydration of each clinker phase analyzed by quantitative X-ray powder diffraction (XRD; C_3S, 0.95; C_2S, 0.74; C_3A, 0.96; C_4AF, assumed as 1.0, total: 0.89), and the CO_2 concentration of the mortar (analyzed as 161.96 mol/m^3). With the corresponding concen-

* Corresponding author. Tel.: +49-531-391-5419; fax: +49-531-391-8179. *E-mail address*: f.schmidt-doehl@tu-bs.de (F. Schmidt-Döhl)

0008-8846/99/$ – see front matter
PII: S0008-8846(99)00094-0

Table 1
Mixture proportions of mortar and concrete

	Mortar	Concrete
Cement	Portland cement PZ 35 F (CEM I 32.5 R), 470.6 kg/m^3	Blast furnace slag cement HOZ 35 L HS/NW/NA (CEM III/B 32.5), 425 kg/m^3
Water/cement ratio	0.6	0.45
Aggregate	Quartz 0–3 mm (near the optimal grain size distribution) 1461.4 kg/m^3	A/B (DIN 1045) 0–16 mm, 1757 kg/m^3

trations the simulation program calculates the phase assemblage of the uncorroded mortar (Table 2, see [2] for details of analytical procedures). If the Fe-end-member of the ettringite solid solution is not considered in thermodynamic calculations, an ettringite concentration of 43.8 mol/m^3 is calculated (lower Al concentration in AFm). In the case of the sandstone the calcitic binder is the only reactive phase. A concentration of 9563 mol/m^3 $CaCO_3$ was measured by differential thermal analysis/thermogravimetry (DTA/TG).

In order to estimate the initial reactive phase assemblage of the concrete, we used the mixture proportions (Table 1) and the chemical compositions of the portland cement clinker and the calcium sulfate. We assumed total hydration of these components. We used the chemical composition of the blast furnace slag and assumed a degree of hydration of 0.25 [4]. We assumed that all Mg in the hydrated cement is bound in a hydrotalcite-type phase with a Al/Mg ratio of 0.38 [4] and subtracted it from the reactive phase assemblage because there are no thermodynamic data for such phases. With this calculated chemical composition, we started the simulation program and obtained an approximate phase assemblage of the uncorroded concrete (C-S-H, AFm, AFt, and a very small but thermodynamically stable amount of $Ca(OH)_2$).

1.3. Thermodynamic data, mixing properties, and Pitzer parameters

The program requires the Gibbs free energy of formation from the elements ΔG^0_{298} of all species that should be considered during the simulation. For simulations with temperatures unequal to 25°C, the heat of formation ΔH^0_{298}, the entropy S^0_{298}, and the function $C_p = f(T)$ are needed. For pressures other than atmospheric at least the molar volume is required. The thermodynamic data used here are taken from Babushkin et al. [5], Taylor [4], Weast et al. [6], Bermann [7], and Robie et al. [8]. We assembled a database of 256 species. Critical comments on these data are advisable.

1. In the case of the CO_2-free hydration of the cement mortar, the ettringite-monosulfate conversion is only calculable if the CAH and CFH species are removed from the database. Otherwise no monosulfate is formed.
2. The authors prefer the data of Al-ettringite from Babushkin et al. [5]. The data cited by Taylor [4] lead to unrealistic SO_4^{2-} concentrations in the pore solution.
3. The formula $CaO \cdot Al_2O_3 \cdot CaCO_3 \cdot 11H_2O$ in the database of Babushkin et al. [5] must be wrong. The correct formula must be: $3CaO \cdot Al_2O_3 \cdot CaCO_3 \cdot 11H_2O$.
4. It was not possible to calculate the stabilization of ettringite and the formation of $3CaO \cdot Al_2O_3 \cdot CaCO_3 \cdot 11H_2O$ in the case of the hydration of a CO_2-containing cement [9] by using the data of Babushkin et al. [5]. Therefore, we changed ΔH^0_{298} of $3CaO \cdot Al_2O_3 \cdot CaCO_3 \cdot 11H_2O$ to 8267.53 kJ/mol. This value corresponds to that of $3CaO \cdot Al_2O_3 \cdot CaCO_3 \cdot 10.68H_2O$ cited by Taylor [4] and changed to 11 H_2O per formula unit.
5. ΔH^0_{298} of Fe_2O_3 was reduced by 20 kJ/mol. The cited data refer to crystalline material. In cementitious materials there is only amorphous Fe_2O_3 at normal temperatures.

All simulations were performed on the assumption of an ideal and complete miscibility of C-S-H end-members. The AFt and AFm-phase were treated in the same way. This is only an approximation [4]. An example of the species considered during the simulations is given subsequently.

For the calculation of the activity coefficients of the solved species and the solvent, the Pitzer parameters of the ions and solved neutral species are required. We used the data presented by Pitzer [10], Reardon [11], and Duchesne and Reardon [12]; however, we prefer the data of Reardon and Duchesne and Reardon.

1.4. Data referring to chemical kinetics

To determine a set of rate constants k for the simulation program, we used suspensions of pulverized, well-hydrated

Table 2
Reactive phase assemblage of the uncorroded mortar at 75% relative humidity (C_s-$CaSO_4$, Cc-$CaCO_3$)

Phase	Concentration in mol/m^3		Comments, calculated solid solutions
	Calculated	Analyzed	
C-S-H	1466.5		$C_{1.87}SH_{1.05}$ (without adsorbed water)
AFm	207.1		$C_3A_{0.88}F_{0.12}Cs_{0.23}Cc_{0.77}H_{11.23}$
$Ca(OH)_2$	857.5	866.43	Analyzed by DTA/TG
Ettringite	46.8	35.4	Analyzed by XRD, $C_3A_{0.51}F_{0.49}Cs_3H_{32}$
H_2O	6801.0		Desorption-isotherm 75% relative humidity

Table 3
Rates of several corrosive reactions

323.2-g pulverized cement paste with a specific surface of 8170 cm^2/g (Blaine) and 840.4 mL NaOH/KOH solution (0.116 m NaOH and 0.254 m KOH) in l-ℓ suspension		
Corrosive substance per 100 mL suspension	k in 10^{-11} m/s	Temperature in °C
Na_2SO_4, 16.07 g	7.73	24.5 ± 0.3
3.602 M HNO_3, 10.3 mL	13.6	27.0 ± 2.0
NH_4HCO_3, 5.86 g	17.7	25.6 ± 0.3
519.9-g pulverized sandstone with a specific surface of 8910 cm^2/g (Blaine) and 724.1 mL H_2O in l-ℓ suspension		
Corrosive substance per 100 mL suspension	k in 10^{-11} m/s	Temperature in °C
3.602 M HNO_3, 10.1 mL	4.74	27.9 ± 0.3

cement paste (water/cement ratio = 0.4) or sandstone with known surface and mixed them with corrosive substances. The change of the chemical composition of the suspension with time was examined with a conductometer, a pH and Ca^{2+}-sensitive electrode. It was possible to describe most of the processes by a heterogenous reaction of the first order with the approximate reaction rates given in Table 3.

1.5. Transport and porosity parameters required by the simulation program

For the calculation of the water transport coefficient *FKU* (capillary, grad u [1,13]), the liquid absorption coefficient *w* and the free water content u_f (saturation water content without pressure) are needed. See Table 4.

The water sorption isotherms and the water transport coefficients *FDP* (diffusion, grad φ [13]) of the cement mortar and the sandstone were determined experimentally. They are not very important for the corrosion experiments presented here. Therefore, they are not displayed; we refer the reader to other work [2]. For the concrete, the data of Kießl [13] were used.

The Na^+ and K^+ diffusion coefficients of the water-saturated cement mortar and the sandstone were examined by steady-state isothermal diffusion experiments according to Brodersen [14]. Solutions with 0.46 mol/kg NaOH and KOH, respectively, were used in the case of the mortar; solutions with 0.1 mol/kg NaCl and KCl, respectively, in the case of the sandstone. The following diffusion coefficients were measured at 23 °C: mortar—D_{Na}, $4.0 \cdot 10^{-8}$; D_K, $3.3 \cdot 10^{-8}$; sandstone—D_{Na}, $1.5 \cdot 10^{-7}$; D_K, $2.1 \cdot 10^{-7}$ (all in m^2/h). All other diffusion coefficients were determined by multiplying these experimental values with constant factors that approximately describe the different velocity of solved species in aqueous solutions in proportion to the Na^+ diffusion: H^+, 2.06; OH^-, 1.68; CO_2^0, 1.31; K^+, 1.24; $Al(OH)_4^-$, 1.24; $Fe(OH)_4^-$, 1.24; Na^+, 1.00; SO_4^{2-}, 0.85; Ca^{2+}, 0.75; Cl^-, 1.96; NO_3^-, 1.89. In the case of the concrete, we used the chloride diffusion coefficients given by Volkwein [15]. A value of $D_{Cl} = 1.8 \cdot 10^{-9}$ m^2/h was chosen.

For the calculation of the temperature dependence of the diffusion of solved species, we used an activation energy of 45.3 kJ/mol for all negative ions in the case of the mortar and concrete and 22.8 kJ/mol in the case of the sandstone. For all positive ions we used an activation energy of 56.0 kJ/mol in the case of the mortar and concrete and 20.8 kJ/mol in the case of the sandstone. For all solved neutral species we used an activation energy of 17.5 kJ/mol. These values were calculated by the use of the tabulated data of Goto and Roy [16], Page et al. [17], and Brodersen [14].

For calculation of the expansion resulting from sulfate attack, the pore radius distribution is required. The distributions of the mortar and the sandstone are shown elsewhere [2]. Some additional porosity and surface parameters are needed by the simulation program. They are summarized in Table 5. The surface parameters are measured by mercury intrusion porosimetry. It was assumed that capillary suction is restricted to pore radii down to 1 μm and diffusion takes place in all pores fillable at 2-kbar pressure.

Table 4
Liquid absorption coefficient and free water content

Material/liquid	W in kg m^{-2} $h^{-0.5}$	u_f in vol.%
Mortar: Water	1.13 ± 0.05	22.7 ± 0.9
Na_2SO_4 solution (0.44 g/L Na_2SO_4)	1.23 ± 0.11	
Na_2SO_4 solution (44 g/L Na_2SO_4)	1.15 ± 0.01	
Acetic acid-sodium acetate buffer solution	0.96 ± 0.04	
Seepage water from the Braunschweig landfill	0.88 ± 0.22	
Water from an activated sludge tank of the seepage water treatment plant of the Braunschweig landfill	0.73 ± 0.09	
Concrete: water	0.76	15.6
Sandstone: water	0.84 ± 0.17	13.1 ± 3.2

Table 5
Additional porosity and surface parameters necessary for simulation program

Parameter	Mortar	Concrete	Sandstone
ρ, Bulk density of the dry material, g/cm^3	1.98 ± 0.02	2.21	2.08 ± 0.02
ε_w, Total open porosity, vol.%	24.2 ± 0.7	15.8	22.6 ± 0.6
ε_{HG}, Total porosity by mercury intrusion, vol.%	15.0 ± 0.2	10.2	17.0 ± 2.6
ε_v, Air void content, vol.%	2.6	1.15	0.0
$S_{s,dif}$, Surface accessible during a diffusive transport (m^2/g)	5.9		1.6
$S_{s,cap}$, Surface accessible during a capillary transport (m^2/g)	$9.7 \cdot 10^{-4}$		$2.9 \cdot 10^{-2}$

1.6. Other starting values

In order to simulate the changes of the material strength, the simulation program needs the characteristic strength of the solid species β_c. We used the following values for the characteristic compressive strength: 365 N/mm^2 for all C-S-H, AFm, and AFt species; 0.0 for $Ca(OH)_2$; 240 N/mm^2 for $CaCO_3$; and 21 N/mm^2 for gypsum [2] in wet environment. The characteristic compressive strength of amorphous SiO_2 was set to 1150 N/mm^2, which is the compressive strength of transparent fused silica. The reason for the low strength of a cementitious material corroded by acids is not a low characteristic strength of the newly formed amorphous silica, but its very high porosity. Other starting values for the simulation are of course the dimensions of the volume elements, the temperature distribution, and, in the case of an expansive process, the ultimate tensile strain (mortar, 0.135 ± 0.015‰; sandstone, 0.30 ± 0.13‰).

2. Results

2.1. Performance of the corrosion experiments in the laboratory

All corrosion experiments in the laboratory were performed with the apparatus shown in Fig. 1. The cylindrical specimens with a length of 10 cm and a diameter of 3 cm were sealed except for the end surfaces. The contact with the corrosive solution was restricted to one end surface. At the onset of experiments, capillary suction was the main transport process. After saturation of the specimens, the diffusion of solved species was the only transport process. During the mortar experiments the corrosive solution (ca. 4.18ℓ;) was exchanged in short time intervals to keep the chemical composition constant. Experiments with sandstone were usually performed without change of the corrosive medium. Normally, sets of three specimens were taken from the experiment; the specimens were cut into disks of at least 12-mm height. Most of the disks were then cut into cubes with a side length of 12 mm. All corroded specimens were stored at 100% relative humidity. The cubes were examined with respect of their tensile splitting strength and several transport parameters. They were quantitatively analyzed by XRD and DTA/TG.

2.2. Corrosion of mortar in contact with an acetic acid sodium acetate buffer solution

In the case of the mortar the comparison of the analyzed and calculated changes of the phase assemblage was mainly based on portlandite and ettringite profiles because they are readily observed by XRD (001, d = 4.90 Å and 220, d = 5.60 Å respectively). Fig. 2 shows the portlandite profile of the mortar after 102 days (the end of the experiment) in contact with an acid buffer solution (1 mol acetic acid and 0.1 mol sodium acetate in 1 kg water). Portlandite is decomposed by the acid and the correspondence of experiment and calculation is good. The other measured portlandite and ettringite profiles also showed a good correlation between experimental and calculated data (6.9, 22, and 102 days contact with acid). The decomposition of portlandite precedes the decomposition of ettringite. Despite the disintegration, no important changes of the specimens dimensions could be observed because of the residual strength of the corroded material. The tensile splitting strength of the corroded material amounts to 0.1 N/mm^2. The simulation program was able to predict this behaviour. The calculated tensile splitting strength of the corroded material amounts to 0.11 N/mm^2; the disintegrated material was able to sustain the self-weight of specimens.

2.3. Corrosion of mortar in contact with Na_2SO_4 solution

In this case, unlike acid attack, a simulation of the corrosion process was only possible if the chemical kinetics of

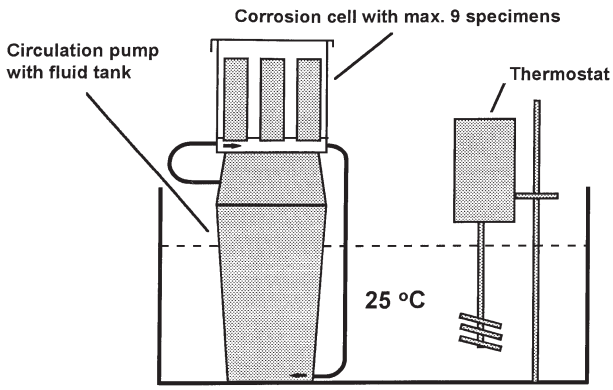

Fig. 1. Apparatus for the corrosion experiments in the laboratory.

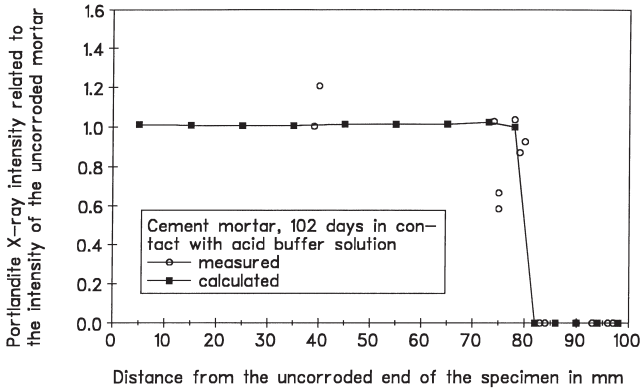

Fig. 2. Portlandite profile of the mortar specimens corroded by an acid buffer solution.

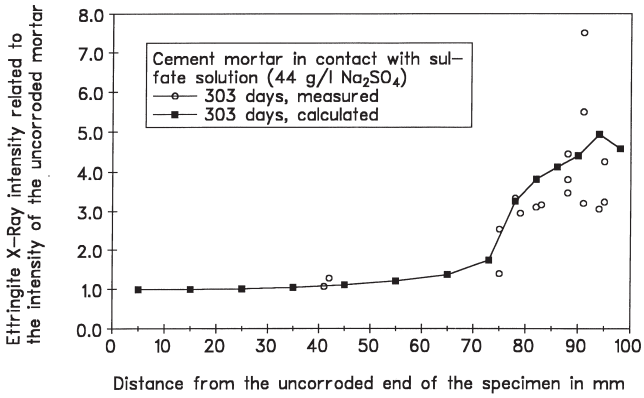

Fig. 4. Ettringite profile of the mortar specimens corroded by Na_2SO_4 solution (44 g/L Na_2SO_4).

ettringite formation were considered. Figs. 3 and 4 show the ettringite profile of the mortar after 154 and 303 days (the end of the experiment), respectively, in contact with a solution of 44 g/L Na_2SO_4. Additional formation of ettringite has taken place and the correspondence between experiment and calculation is good. After 39 days the profile of ettringite and all portlandite profiles (39,154,303 days) showed a good correlation between experimental and calculated data also. After 303 days gypsum was formed at the corroded side of the specimens. This was also predicted by the simulation program.

Fig. 5 shows the measured and calculated expansion of the mortar specimens (changes of diameter). There is a satisfying correspondence. The transport processes examined in the laboratory experiments were one-dimensional. Therefore it was possible to make an exact comparison of measured expansion and concentration profiles. Figs. 3, 4, and 5 show that the expansion was locally and temporally related to the ettringite concentrations within the specimens. The expansion stopped as soon as the specimens were removed from the sulfate solution and stored at 100% relative humidity.

Fig. 5 shows that the expansion increases until the corroded end of the specimen, although the ettringite concentration at the corroded end stagnated at the maximal possible amount (Fig. 4). In our opinion this is a lever effect of the zone in which the new formation of ettringite is active. This lever effect results in a wide opening of cracks at the corroded end of the specimens.

During this experiment a decreasing material strength and an increasing porosity ϵ_{HG}, water absorption coefficient (w), and free water content u_f within the corroded part of the specimens were observed because the expansion destroyed the material structure and led to increased cracking. The simulation was not able to calculate these parameters correctly. The discrepancy between the calculated and measured diffusion coefficients within the corroded material was, however, small.

In contact with a solution of 0.44 g/L Na_2SO_4 the mortar showed only little newly formed ettringite. The correspondence of measured and calculated concentration profiles was not as good as in the experiment with 44.0 g/L Na_2SO_4 but the correspondence became better with time. Fig. 6 shows the ettringite profile of the mortar after 301 days (the end of the experiment), depicted with the same scale as in Figs. 3 and 4. No expansion or other indications of chemical attack were measured or calculated.

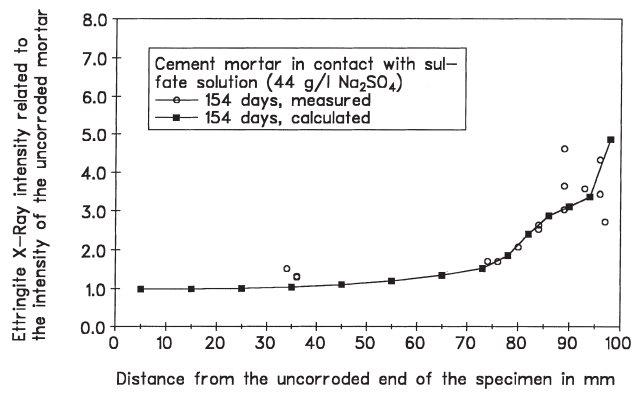

Fig. 3. Ettringite profile of the mortar specimens corroded by Na_2SO_4 solution (44 g/L Na_2SO_4).

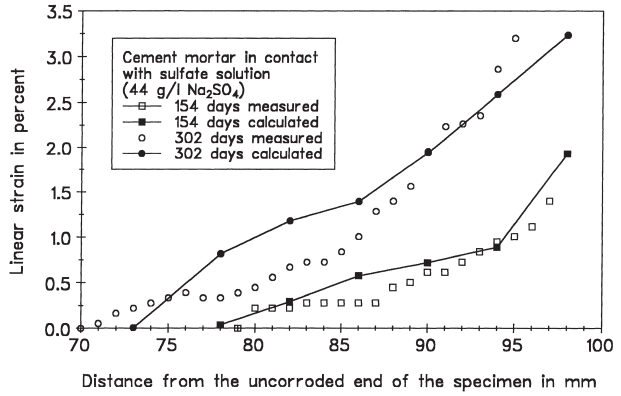

Fig. 5. Expansion of the mortar specimens corroded by Na_2SO_4 solution (44 g/L Na_2SO_4).

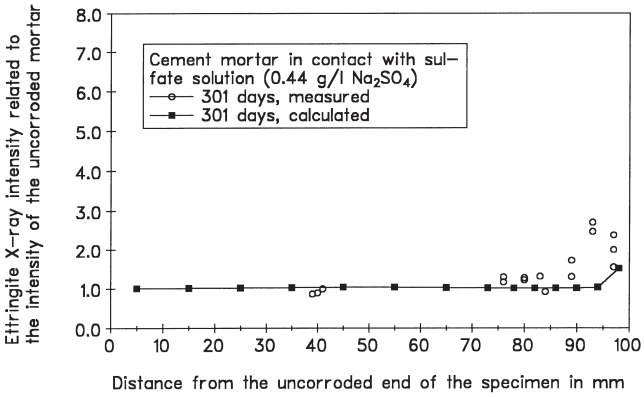

Fig. 6. Ettringite profile of the mortar specimens corroded by Na_2SO_4 solution (0.44 g/L Na_2SO_4).

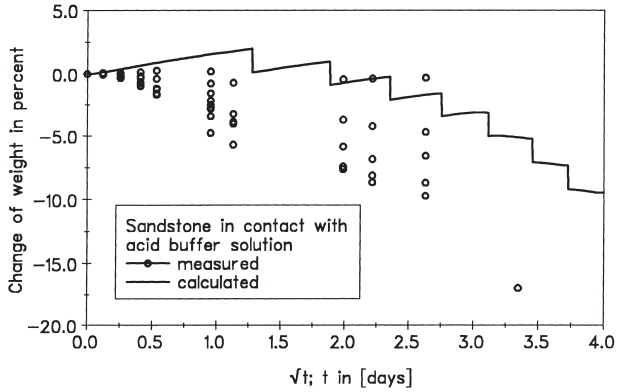

Fig. 7. Loss of mass of the sandstone specimens corroded by an acid buffer solution.

The following species were considered during these simulations:

$C_2SH_{1.17}$, $C_3S_2H_3$, $C_4S_3H_{1.5}$, C_6S_6H, $C_5S_6H_3$, $C_5S_6H_{5.5}$, $C_5S_6H_{10.5}$, CS_2H_2, $C_2S_3H_{2.5}$,
C_3S, βC_2S, C_3A, C_4AF, $3CaO \cdot Al_2O_3 \cdot 3CaSO_4 \cdot 32H_2O$, $3CaO \cdot Fe_2O_3 \cdot 3CaSO_4 \cdot 32H_2O$,
$3CaO \cdot Al_2O_3 \cdot CaSO_4 \cdot 12H_2O$, $3CaO \cdot Al_2O_3 \cdot CaCO_3 \cdot 11H_2O$, $3CaO \cdot Fe_2O_3 \cdot CaSO_4 \cdot 12H_2O$,
H_2O, KOH, NaOH, $Ca(OH)_2$, Na_2O, K_2O, CO_2 (gas),
FeOOH (lepidocrocite), $Fe(OH)_3$ (amorph), Fe_2O_3, AlOOH (boehmite), $Al(OH)_3$ (amorph), Al_2O_3,
$CaCO_3$ (calcite), $CaCO_3$ (aragonite), $CaSO_4$, $CaSO_4 \cdot 2H_2O$, $Na_2SO_4 \cdot 10H_2O$,
H^+, K^+, Na^+, Ca^{2+}, $CaOH^+$, OH^-, SO_4^{2-}, CO_3^{2-}, HCO_3^-, $Al(OH)_4^-$, $Fe(OH)_4^-$, CO_2^0

2.4. Corrosion experiments with mortar and concrete in a seepage water treatment plant

The concentrations in the seepage water from the Braunschweig landfill are shown in Table 6. We immersed mortar (up to 74 days) and concrete (up to 545 days) specimens (see Table 1) in several tanks of the seepage water treatment plant. To our surprise we found no corrosive effect even in the untreated water. Consequently, we investigated the corrosion behaviour with the simulation program. This investigation rendered the same result. The simulations showed that the high concentration of HCO_3^- is responsible for mitigating ammonium attack.

2.5. Corrosion of sandstone in an acid buffer solution with and without Na_2SO_4

The sandstone specimens showed a rapid ablation in contact with the acid buffer solution described above: the calcitic binder was completely destroyed. Fig. 7 shows the measured and the calculated loss of mass, which is directly related to the shortening rate. Most of the specimens showed a loss of weight that was greater than the weight increase by the capillary suction. The dispersion of the material behaviour of this natural stone is quite large. The reason for the stepwise form of the calculated curve is that, in the case of an acid attack with a shortening of the specimen, the simulation program removed single volume elements from the structure. Whenever a volume element is removed, the mass of the specimen is decreased by the mass of the unreactive material within the volume element. To approximate the continuous process, the lower corners must be connected. The calculated curve is located within the experimental values but not close to the central value.

To examine the formation of gypsum, we mixed the acid buffer solution with Na_2SO_4 (992 mL of buffer solution and 40 g/L of Na_2SO_4 in 1 L of solution). In contact with this solution the calcitic binder of the sandstone changed into gypsum. The chemical reaction led to a decrease of strength of the corroded material but there was only a very slow ablation of the specimens. The calculated dimension of the gypsum-rich area was located within the measured values (4–8 mm after 42 days), but the calculated gypsum concentration was only about 60% of the measured DTA/Th. We do not know the reason for that.

3. Conclusions

The comparison of the corrosion experiments and the computer simulations show that the chemical reactions were correctly predicted in any case. The changes of the phase assemblage and the dimension of damage were quantitatively

Table 6
Average ion concentrations in the untreated seepage water from the Braunschweig landfill

Ion	NH_4^+N	NO_3^-N	Cl^-	Na^+	K^+	Mg^{2+}	Ca^{2+}	HCO_3^-	SO_4^{2-}	pH
Concentration mg/L	912	26.2	1779	1787	1349	135	121	8495	140	8.17

calculable in most cases. Whether the corroded material is mechanically stable or if a considerable loss of mass from the corroded surface takes place could be simulated on the basis of the strength of the corroded material. The expansion of a cement mortar in the case of the attack by a Na_2SO_4 solution was calculable. The prediction of some structure-dependent parameters in the case of cracking was difficult and not always correct. The comparison of the measured and calculated corrosion behaviour of the examined materials lead to the conclusion that the algorithm is able to simulate very different corrosion processes without any change of the model despite some difficulty in detail.

In the meantime the simulation program is able to simulate two-dimensional transport processes. The program was designed to simulate the chemical attack on structural components (in particular, concrete components) by aqueous solutions in the case of a single episode of exposure (transport processes restricted to diffusion of solved species after an initial period). Such components are piles, foundations, tanks, pipes, and others. In addition to the previously published material [1,2], it is now also possible to use the model of Künzel [18] for the calculation of heat and moisture transport processes. Therefore, simulations of chemical attack with wetting and drying cycles are now possible but should be interpreted cautiously because changes of some transport parameters during the corrosion process are difficult to simulate (e.g., the parameters that determine the capillary transport processes).

Acknowledgments

The authors would like to express their thanks for the financial support by the Deutsche Forschungsgemeinschaft.

References

[1] F. Schmidt-Döhl, F.S. Rostásy, Cem Concr Res (submitted for publication).
[2] F. Schmidt-Döhl, Ein Modell zur Berechnung von kombinierten chemischen Reaktions- und Transportprozessen und seine Anwendung auf die Korrosion mineralischer Baustoffe, Institut für Baustoffe, Massivbau und Brandschutz der Technischen Universität Braunschweig, H. 125, 1996.
[3] W.-D. Grimm, Bildatlas wichtiger Denkmalgesteine der Bundesrepublik Deutschland. Arbeitsheft 50 des Bayerischen Landesamtes für Denkmalpflege, München, 1990.
[4] H.F.W. Taylor, Cement Chemistry, Academic Press, London, 1990.
[5] V.J. Babushkin, G.M. Matveyev, O.P. Mchedlov-Petrossyan, Thermodynamics of Silicates, Springer Verlag, Berlin, 1985.
[6] R.C. Weast, M.J. Astle, W.H. Beyer, CRC Handbook of Chemistry and Physics, 66th ed., CRC Press, Boca Raton, 1986.
[7] R.G. Bermann, Internally-consistent thermodynamic data for minerals in the system Na_2O-K_2O-CaO-FeO-Al_2O_3-SiO_2-TiO_2-H_2O-CO_2, J Petrology 29 (1988) 445–522.
[8] R.A. Robie, B.S. Hemingway, J.R. Fisher, Thermodynamic properties of minerals and related substances at 298.15 K and 1 Bar (10^5 Pascals) pressure and at higher temperatures, US Geol Surv Bull 1452, 1979.
[9] H.-J. Kuzel, H. Meyer, Mechanism of ettringite and monosulfate formation in cement and concrete in the presence of CO_3^{2-}, Proc. 15th Int. Conf. Cem. Microscopy, Dallas, TX, 1993, 191–203.
[10] K.S. Pitzer (ed.), Activity coefficients in electrolyte solutions, 2d ed., CRC Press, Boca Raton, 1991.
[11] E.J. Reardon, An ion interaction model for the determination of chemical equilibrium in cement/water systems, Cem Concr Res 20 (1990) 175–192.
[12] J. Duchesne, E.J. Reardon, Measurement and prediction of portlandite solubility in alkali solutions, Cem Concr Res 25 (1995) 1043–1053.
[13] K. Kießl, Kapillarer und dampfförmiger Feuchtetransport in mehrschichtigen Bauteilen. Rechnerische Erfassung und bauphysikalische Anwendung, Doctoral Thesis, Universität Essen (Gesamthochschule), 1983.
[14] H.A. Brodersen, Zur Abhängigkeit der Transportvorgänge verschiedener Ionen im Beton von Struktur und Zusammensetzung des Zementsteins, Doctoral Thesis, Technische Universität Aachen, 1982.
[15] A. Volkwein, Untersuchungen über das Eindringen von Wasser und Chlorid in Beton, Doctoral Thesis, Technische Universität München, 1991.
[16] S. Goto, D.M. Roy, Diffusion of ions through hardened cement pastes, Cem Concr Res 11 (1981) 751–757.
[17] C.L. Page, N.R. Short, A. El Tarras, Diffusion of chloride ions in hardened cement paste, Cem Concr Res 11 (1981) 395–406.
[18] H.M. Künzel, Verfahren zur ein- und zweidimensionalen Berechnung des gekoppelten Wärme- und Feuchtetransportes in Bauteilen mit einfachen Kennwerten, Doctoral Thesis, Universität Stuttgart, 1994.